



Regional Gravity Field Model of Egypt Based on Satellite and Terrestrial Data

MOHAMED SOBH,^{1,2} AHMED HAMDI MANSI,^{3,4} SIMON CAMPBELL,⁵ and JÖRG EBBING¹

Abstract—This study presents a recent combined regional gravity field model over Egypt, developed by integrating satellite and terrestrial data via applying the remove-compute-restore (RCR) principle and the least-squares collocation (LSC) procedure. A high-resolution digital terrain model was exploited for the computation of the terrain and residual terrain corrections. Hereby, all the signals that can be modelled or deterministically computed are considered known and then removed in order to reduce the order of magnitude of the input gravity data prior to applying the LSC. Several GOCE-only and combined global geopotential models (GGMs) have been thoroughly investigated with respect to the EGM2008, in which the space-wise (SPW) solution, namely the SPW-R5 model, demonstrated the best performance. For the development of the combined model, the SPW-R5 GGM has been integrated with both the EGM2008 GGM and the terrestrial data retrieved from 56,250 gravity stations of the Getech data, acquired in the framework of the African Gravity Project. The combined regional gravity model was compared to the state-of-art XGM2016 global gravity model. The standard deviation of the differences is 18.0 mGal in terms of Bouguer anomalies. The combined regional model fits well with the terrestrial gravity data along the chosen North–South oriented profile through the Nile Delta region. The improvements of the developed combined regional model over the XGM2016 are due to the use of a more extensive terrestrial dataset. In conclusion, our model is more suitable than solely using the ground data or GGMs for regional density modelling over Egypt. As an example, the comparison of using a global or regionally defined gravity model with the forward gravity modelling based on Saleh (*Acta Geodaetica et Geophysica Hungarica* 47(4):402–429, 2012) density model is performed.

Key words: GOCE-based models, remove-compute-restore (RCR), XGM2016, combined gravity model, density modelling.

1. Introduction

High-resolution regional gravity field models are of a great importance for both geophysical and geo-dynamical applications, e.g. reliable density structure modelling of the crust and lithosphere (Shih et al. 2015; Sampietro et al. 2018). Such a high-resolution gravity model can be typically estimated from terrestrial gravity measurements, which are not always available with a suitable coverage density. On the other hand, the global geopotential models (GGMs) derived from satellite observations can only contribute the long wavelength signal.

There is a distinction between satellite-only models, e.g. the Laser Geodynamics Satellites (Lageos) (Yoder et al. 1983), CHAllenging Minisatellite Payload (CHAMP) (Reigber et al. 1999), Gravity Recovery And Climate Experiment (GRACE) (Tapley et al. 2004), and, recently, the Gravity Field and Steady-State Ocean Circulation Explorer (GOCE) (Drinkwater et al. 2003; European GOCE Gravity-Consortium 2010), and combined ones. Currently, several different combined GGMs such as the Gravity Observation Combination solutions (GOCO) (Pail et al. 2010), the European Improved Gravity models of the Earth by New techniques (EIGEN6C4) (Förste et al. 2014), and the GOCE and EGM2008 combined model (GECO) (Gilardoni et al. 2016) have been produced. These models comprise non-homogeneous terrestrial datasets, which are reflected as biases and distortions within the final gravity field model (Gatti et al. 2013). On the one hand, in the last decade, the International

¹ Institute of Geosciences, Christian-Albrechts-Universität Kiel, Otto-Hahn-Platz 1, 24118 Kiel, Germany. E-mail: mohamed.sobh@ifg.uni-kiel.de; joerg.ebbing@ifg.uni-kiel.de

² Geodynamics Department, National Research Institute of Astronomy and Geophysics (NRIAG), Helwan, Cairo 11421, Egypt.

³ Istituto Nazionale di Geofisica e Vulcanologia, sezione di Pisa, Via U. della Faggiola 32, 56126 Pisa, PI, Italy. E-mail: ahmed.mansi@ingv.it; ahmed.hamdi@polimi.it

⁴ Department of Civil and Environmental Engineering, Politecnico di Milano, Piazza Leonardo da Vinci 32, Milan, Italy.

⁵ Gravity and Magnetic solutions, Getech UK, Kitson House, Elmete Hall, Elmete Lane, Leeds LS8 2LJ, UK. E-mail: simon.campbell@getech.com

Association of Geodesy (IAG) has been interested in establishing a reliable geoid for the African continent as a whole [for instance, see Abd-Elmotaal et al. (2018)], where the Getech data, utilised in the current research, were not available), and accurate local/regional geoids for each state. For the geoid determination and geodetic applications, the interested reader is referred to Alnaggar (1986), Hanafy and El Tokhey (1993), Abd-Elmotaal (2008) and Dawod (2008). In particular, the terrestrial gravity data over Egypt suffer large data gaps as well as being heterogeneously distributed, which lead to a low-resolution gravity field model, which, in turn, is not practical for a reliable density structure modelling. Consequently, for Egypt and similar regions, there is a persistent need to develop high-resolution regional combined gravity models based, mainly, on the recently made available terrestrial gravity data.

Hence, the best-fitting regional gravity models are derived by implementing the Remove-Compute-Restore (RCR) procedure and the Least-Squares Collocation (LSC) algorithm to integrate the available ground-based gravity data (Sect. 2.1) with GOCE-based GGMs (Sect. 2.2).

As a preliminary step, the GOCE-based GGMs were evaluated/assessed using independent ground-based gravity data in order to exclusively concentrate on those models that closely describe the gravity field over Egypt and to understand within which spectral bands they deliver improved information. Accordingly, after the evaluation and modelling processes, the capabilities of the developed combined model were assessed by forward-compute the Bouguer anomaly field along a North–South oriented transversal profile that passes through the Nile Delta region based on the well-constrained density model proposed by Saleh (2012).

This paper is organized as follows: Sect. 2 gives a brief description of the various utilised datasets. Then, the methodology to evaluate the performance of GOCE-based GGMs with respect to the XGM2016 (Pail et al. 2016) model and terrestrial gravity data is reviewed in Sect. 3. Section 4 reviews the computation of the regional gravimetric model, integrating the terrestrial data, the SPW-R5 solution, and the EGM2008 global model, via the RCR method and LSC algorithm. Section 5 discusses the model

validation, whereas details on the forward density modelling process are given in Sect. 6. Finally, some relevant conclusions regarding the assessment of the regional gravity modelling using combined GOCE-based data and terrestrial gravity observations are drawn in Sect. 7.

2. Datasets

The datasets used in this study consist of (1) terrestrial free-air (FA) gravity anomalies, (2) gravity field in terms of gravity anomalies derived from the GOCE-based GGMs and the XGM2016 (Pail et al. 2016) model, and (3) high-resolution ($3'' \times 3''$ arc-second) topographic heights provided in terms of a digital terrain model (DTM) over the study area.

2.1. Terrestrial Gravity Data

A regular $5' \times 5'$ arc-minute grid of FA gravity anomalies, extended over Egypt, was provided by the Getech. This grid was developed using a simple interpolation algorithm over the 56,250 observation stations, acquired in the framework of the African Gravity Project (Fairhead et al. 1988). Figure 1 shows the distribution of those gravimetric stations projected onto a topographic map. As some of these data were collected long before the GNSS/GPS era, the major sources of errors that contaminate the data are the inaccurate estimates of the positions and heights of the stations. For most surveys, details on the accuracy and/or errors are neither separately provided nor reported within the acquisition logs metadata. The data provider has suggested an accuracy of 1.0 mGal. However, it is expected that the accuracy of the provided FA gravity anomalies based on the noticeable high-inhomogeneity should be substantially lower in the majority of the study area.

Since the processing of the Getech gravity data is not clearly understood, by the common user, and that the data provider recommends the 1.0 mGal accuracy, it is difficult to assess the actual accuracy of the data used for creating the FA grid. However, considering that the BGI (Bureau Gravimétrique International) gravity data over the Egyptian territory have been included for the generation of the previous

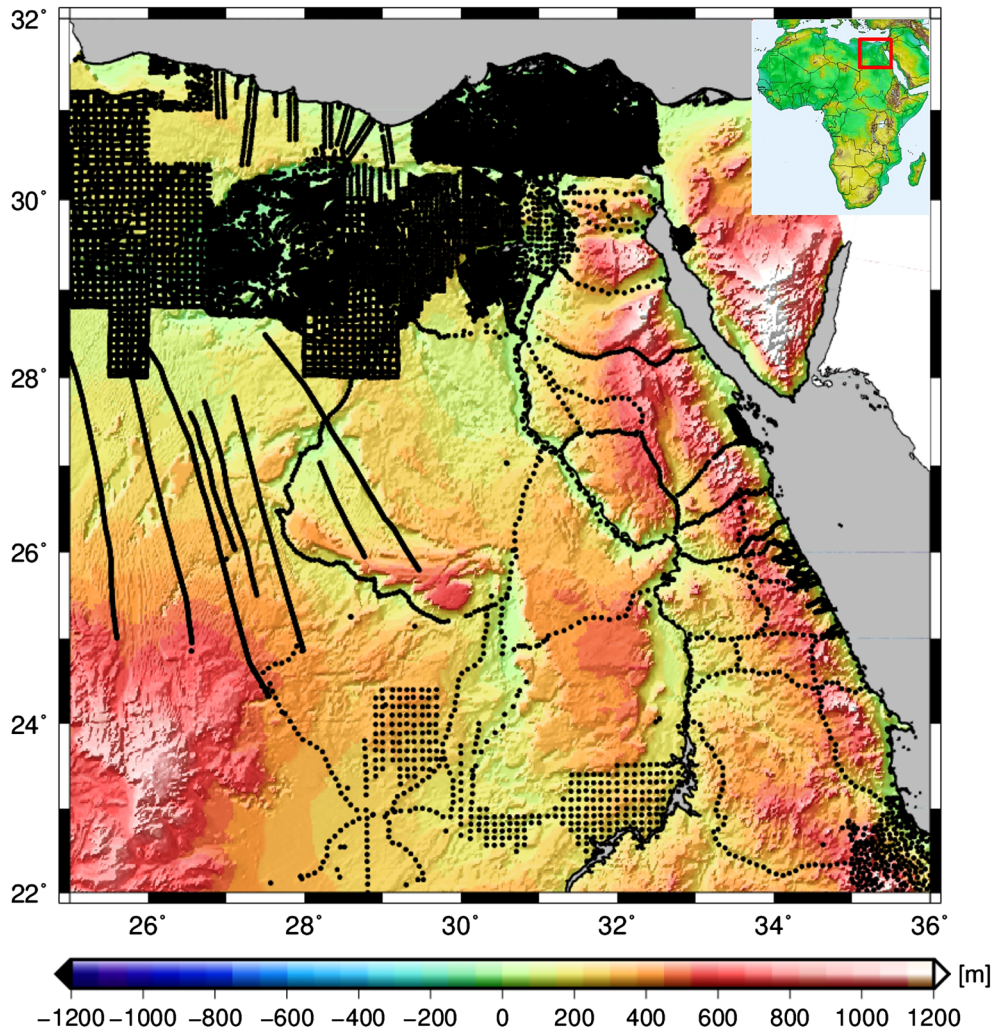


Figure 1

The spatial distribution of the available terrestrial gravity stations over Egypt projected onto a topographic map; unit [m]

$5' \times 5'$ arc-minute grid of gravity anomalies, we have attempted to assess the prediction accuracy by comparing each validated BGI gravity observation with its corresponding Getech grid-based predicted value using the Spline interpolation. Figure 2a shows the spatial distribution of the 320 BGI gravity stations used for such a validation. The residuals range between -20.83 and 20.26 mGal with a mean value of about -0.43 mGal and a standard deviation (STD) of 7.01 mGal. Figure 2b shows the histogram of the Getech grid data evaluation, where the residuals show a Gaussian normal distribution. The analysis of the results proves that such a gridded gravity dataset is

suitable for geophysical applications such as the purpose of this research, i.e. regional density modelling.

2.2. GOCE-Based GGMs and XGM2016

The various existing GOCE-based GGMs are globally optimized; therefore, they, generally, exhibit similar characteristics when the gravitational signal is analysed on a global scale. Still, these models can differ, especially, when the gravity field is studied on a local or regional scale. Hence, three recent GOCE-based GGMs, based on the space-wise (SPW) (Gatti

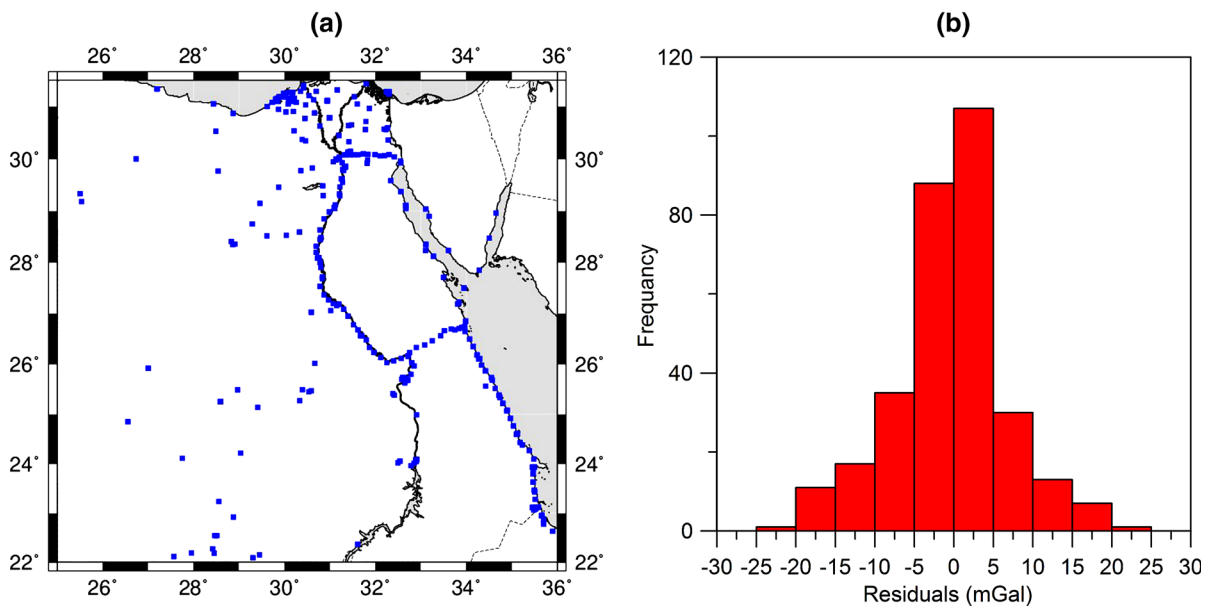


Figure 2

a The spatial distribution of the 320 BGI gravity stations; unit [$^{\circ}$] and **b** the histogram of the discrepancies between the BGI dataset and the Getech-based predicted values; unit [mGal]

et al. 2016), direct-wise (DIR) (Bruinsma et al. 2013), and time-wise (TIM) (Pail et al. 2010) approaches, have been utilized in order to cross-validate the terrestrial FA gravity anomalies. While the development of the SPW-R5 solution exploited the full GOCE gradiometry mission, both the DIR-R5 and TIM-R5 solutions only used about 42 months of GOCE measurements. In detail, the latter, namely the TIM-R5, has been considered the core data in developing the GOCO5S combined model (Mayer-Gürr et al. 2015). These models are available in terms of spherical harmonic (SH) coefficients. For more details about the model differences, see Pail et al. (2011).

The XGM2016 model (Pail et al. 2016) has been used as the state-of-the-art high-resolution GGM in order to assess the considered GOCE-only as well as combined GGMs. The XGM2016 is a preparation release of the planned Earth Gravitational Model 2020 (EGM2020) that will succeed the EGM2008 (Pavlis et al. 2008). For instance, the XGM2016 combines recent terrestrial gravity data with the latest satellite gravity observations from GRACE, GOCE,

and altimetry up to a maximum SH degree/order (d/o) of 719.

2.3. Digital Terrain Model

The availability of a high resolution DTM is essential when locally/regionally comparing GOCE-based GGMs with the terrestrial gravity data since it would be used to fill in the remaining gravity signals beyond those provided by the maximum d/o of GOCE-based models by computing the so-called Residual Terrain Model (RTM) (Forsberg 1984). The topographic heights collected by the Shuttle Radar Topography Mission (SRTM) with a resolution of 3" arc-second (≈ 90 m), shown in Fig. 1, have been used. Such data are freely distributed via the public web service (<https://lta.cr.usgs.gov/SRTM>) (Farr et al. 2007). Due to the low resolution of the terrestrial gravity data, equivalent to 5' arc-minute, the 3" arc-second spatial resolution DTM was preferred over the other available high-resolution products, e.g. the 1" arc-second, in order to avoid the propagation of any uncorrected artefacts (Walker et al. 2007; Arrell et al. 2008).

3. Processing Strategy

3.1. Overview

The processing scheme that consists of three main steps, in which the output of one step will serve as the input to the succeeding one, is explained as follows:

1. Comparison: cross-compare the performance of the investigated GOCE-based GGMs, the XGM2016, and the terrestrial FA gravity signals, where the latter takes the terrain reduction, i.e. the RTM method, into consideration;
2. Regional modelling: the gravity field, sewing together the ground observations, GOCE-based SPW solution, and the EGM2008 model, is estimated on the basis of the RCR method and LSC technique;
3. Validation: the performance of the combined regional gravity model is validated using the high-resolution XGM2016 GGM and the well-constrained density model built for a transversal profile oriented North–South along the Nile Delta region.

To decide which of the investigated GOCE-based GGMs would better model the gravity field over Egypt, the synthesized signals, at least in theory, must be validated using gravity-independent data (e.g. seismic data). In practice, both the XGM2016 and a few independent gravity stations that took the spectral consistency into consideration, i.e. the short and very short wavelengths signals beyond the maximum d/o of the GOCE-based GGMs, were used.

GOCE-based GGMs and the XGM2016 models are cross-compared at the same spectral bands, where their SH syntheses have been constructed from d/o = 2 up to $N_{\max} = 250$ (with a step of d/o = 10). More attention was given to the d/o ranging from 100 to 250, corresponding to a regional spatial resolution that approximately varies between 200 and 80 km (20,000 km/degree), respectively, to examine which GGM closely approximated and better described the gravity field over Egypt, especially at the medium-to-short wavelength spectral bands where they are expected to deliver their improved information (Bruinsma et al. 2013; Sampietro et al. 2018).

The performance of the various investigated GOCE-based GGMs and the EGM2008, with respect to a reference model, for instance, the XGM2016, in terms of degree difference amplitude ($\Delta\sigma_n$) is presented in Fig. 3. Such differences have often been computed in order to quantify the powers of the signal and its corresponding gravity field estimation error at various spatial wavelengths using Eq. (1).

$$\Delta\sigma_n = \frac{GM}{R_E^2} \cdot \sqrt{\sum_{m=0}^n (\Delta c_{nm}^2 + \Delta s_{nm}^2)} \quad (1)$$

where G is the Newtonian gravitational constant, M is the bulk-mass of the Earth, Δc_{nm} and Δs_{nm} are the differences of the SH sine and cosine coefficients between the GOCE-based GGMs and the corresponding ones of the XGM2016, n and m are the SH degree and order, respectively, and R_E is the mean radius of the Earth at the reference ellipsoid $\equiv 6378.137$ km.

From d/o 200 onward, the monotonic STD has rapidly increased for all the GOCE-based GGMs solutions, since the coefficients beyond d/o 180–200 were estimated with the use of Kaula's rule (Kaula 1966) and the signal-to-noise ratio (SNR) noticeably diminished over d/o equivalent to 200 (Rummel 2010). The SPW-R5 GGM, the fifth release of the SPW solution, provides a small degree difference amplitude at lower SH degrees and, on the meantime, outperforms the other two official European Space Agency (ESA) products, namely the DIR-R5 and TIM-R5 solutions, as well as the GOCO5S GGM. The EGM2008 model has the least degree difference amplitudes, especially at higher SH degrees as a direct consequence of the usage of the altimetry/terrestrial data into its development. Therefore, all above-mentioned GOCE-based GGMs will be analysed but only the plots related to processing the SPW-R5 model, expected to deliver the best results, will be plotted.

3.2. Validations and Pre-processing of the Terrestrial Data

As a start, a quality assurance step is necessary as the terrestrial data were acquired over a long time span with different measurement techniques without any quality control/assurance metadata. Therefore,

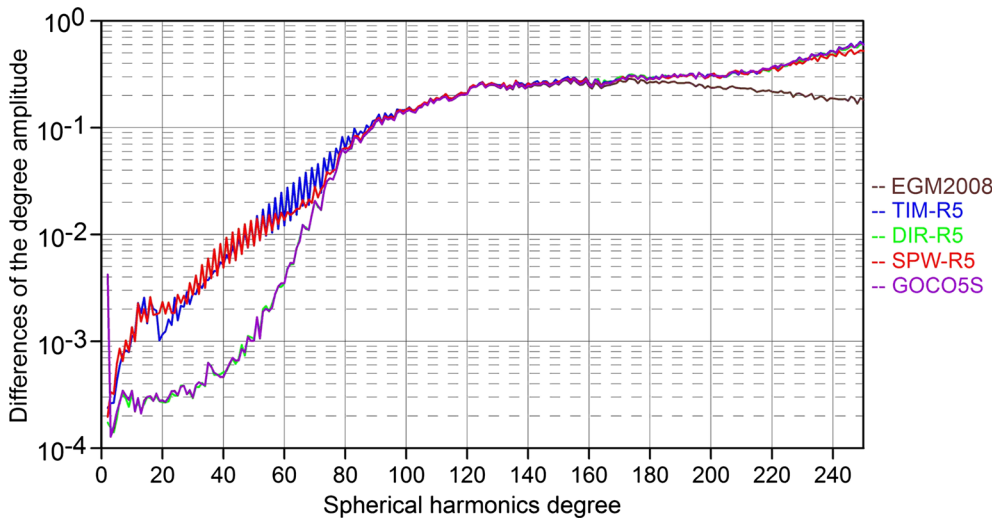


Figure 3

Degree difference amplitude of the gravity field anomalies of the various investigated GOCE-based GGMs as well as the EGM2008 model (from degree/order = 2 to $N_{\max} = 250$) with respect to the corresponding signal from the XGM2016 model truncated at the same spherical harmonics degree/order; unit [mGal]

the data were first cross-validated (i.e. filtered) and the existing outliers were tagged and removed. All the heights of the 56,250 gravity stations were compared with the commensurate ones from the SRTM-based DTM. The height discrepancies range between -685 and 369 m with a mean and STD of 5.9 and 72.9 m, respectively. All gravity stations with height differences beyond ± 100 m, which corresponds to about 30 mGal in terms of FA anomaly values, were flagged and then filtered. Applying such an empirical outlier detection, a total number of 6000 stations were identified and then removed as reported in Fig. 4.

To evaluate the topographic effects by means of RTM, two DTMs were used, namely the detailed and reference ones. The former is the actual high-resolution DTM (a spatial resolution of 3 arc-second), while the latter is a smoothed DTM (of $5'$ arc-minute resolution that is consistent with the spatial resolution of the terrestrial gravimetric data) obtained via applying a moving average window over the detailed one. The two terrain correction signals, exploited to evaluate the RTM, are computed by means of the Gravity Terrain Effects (GTE) software package (Sampietro et al. 2016; Capponi et al. 2017).

The GTE software is an integration of the deterministic prism modelling and fast Fourier transformation (FFT) techniques in order to maximize the accuracy of the computed gravitational effects, at any given altitude as well as the surface of the topography, minimizing the computational time (Sampietro et al. 2016). The topography potential induced by the residual topographical masses between those two DTMs is taken into account within the reduction process (Sampietro et al. 2017; Zaki et al. 2018). The topography effects on gravity in terms of RTM reduction dg_{RTM} are approximated in Forsberg (1984).

First, the syntheses of the investigated GOCE-based GGMs, truncated at various d/o, are compared to the XGM2016 signal, in terms of FA gravity anomalies, where within Table 1, the statistics of only d/o 200 and 240 are reported for the sake of simplicity. The STD of the differences for d/o 200 and 240 are at the level of 0.72 and 2.76 mGal, respectively. Therefore, d/o 200, in which all GGMs delivered the minimum STD values, will be used as the integration SH threshold. Also, the SPW-R5 will be exploited in the development of the combined model as it has illustrated the minimum statistics, in terms of minimum, maximum, and mean error values as well as the lowest STD value.

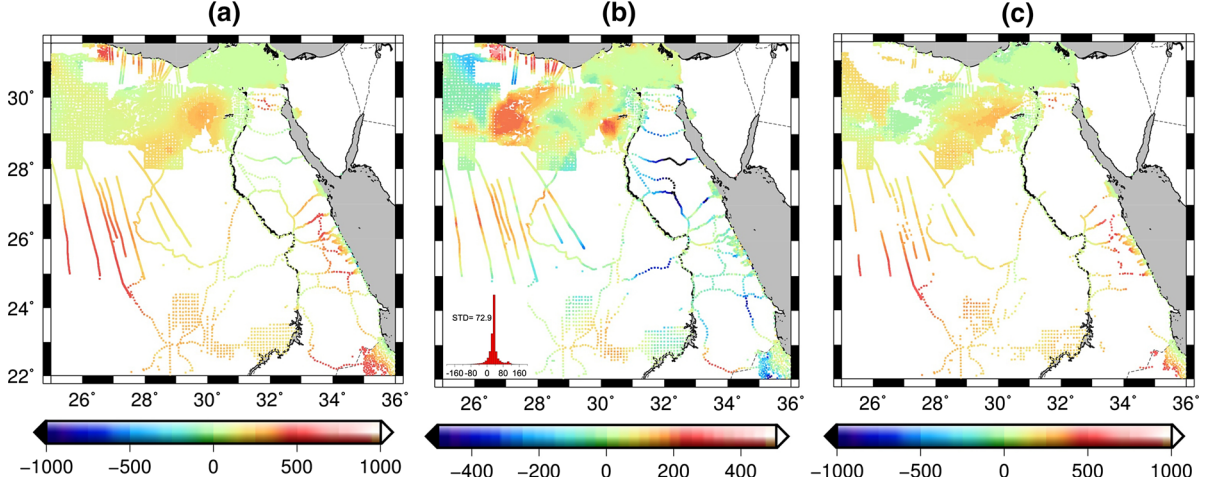


Figure 4

Comparison of gravity station heights provided by the Getech dataset, **a** the absolute heights, **b** the differences to the SRTM-based DTM, where the histogram of these height differences, whose standard deviation equals 72.9 m, is reported on the lower left corner, **c** the remaining heights after the removal of outliers; unit [m]

Table 1

The statistics of the differences between the free-air gravity anomalies obtained from GOCE-based GGMs truncated to degree/order 200 and 240 and the corresponding signal calculated from the XGM2016 model; units [mGal]

Model	$\delta\Delta g_{FA}$ ($N_{max} = 200$)				$\delta\Delta g_{FA}$ ($N_{max} = 240$)			
	Min	Max	Mean	STD	Min	Max	Mean	STD
SPW-R5	-2.86	4.07	0.02	0.72	-10.02	9.59	0.55	2.76
DIR-R5	-3.29	4.49	0.13	0.79	-8.43	8.20	0.25	3.33
TIM-R5	-3.42	4.28	0.07	0.66	-9.13	8.98	0.35	3.41
GOCOSS	-4.64	5.34	0.20	1.40	-16.99	15.81	1.49	6.16

After checking the height information and before the application of the LSC procedure, the acquired gravity values had to be validated. This validation was accomplished by thoroughly comparing the terrestrial observations to the syntheses of the SPW-R5 and XGM2016 GGMs in a restricted spectral bandwidth, up to d/o 200 and 719, respectively, without using the RTM signal. Consequently, the results of the mutual-comparison of the data to the SPW-R5 and XGM2016 are shown in Fig. 5. As expected, the differences resulting from the utilization of the SPW-R5 are high in several regions, because GOCE resolution does not cover the short wavelengths signals. The small differences obtained from the XGM2016 are justified as it contains the

medium-to-short wavelengths. Table 2 documents the main statistical properties of such a validation.

For the sake of completeness, in other cases, where terrestrial data are not dense, or are scarce or where outliers can be expected, Bomfim et al. (2013) attempted to use the GOCE data as a tool for the quality assessment to test terrestrial gravity data in order to improve the data coverage in order to correctly represent the gravity field.

4. Combined Gravity Field Modelling Over Egypt

In order to compute the combined regional gravity model integrating together the available terrestrial

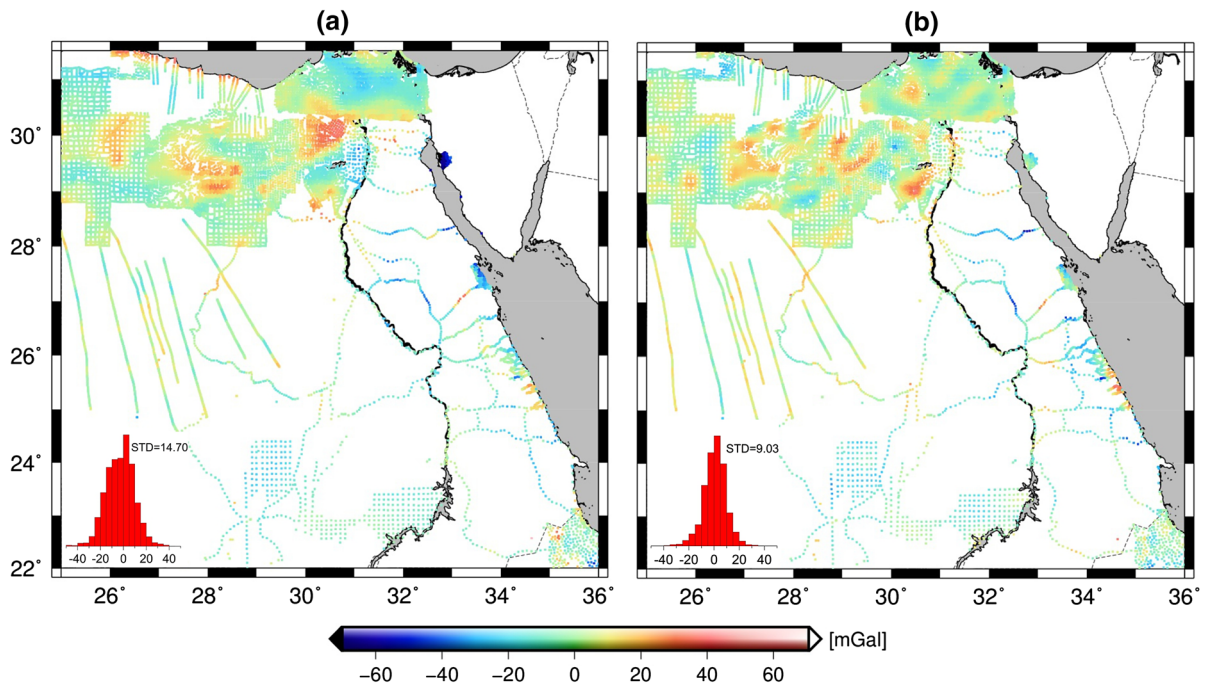


Figure 5

The differences of the terrestrial gravity data with respect to **a** the SPW-R5 synthesized to degree/order 200 and **b** the XGM2016 synthesized to degree/order 719. The histogram of the residuals whose standard deviation is 14.70 and 9.03, respectively, is reported on the lower left corner; unit [mGal]

Table 2

Statistical parameters of the differences between the terrestrial gravity data and the global gravity field synthesised by the SPW-R5 and XGM2016 models up to $N_{\max} = 240$; units [mGal]

Anomaly	Min	Max	Mean	STD
SPW-R5 [d/o 200]	- 78.31	57.90	- 3.90	14.70
XGM2016 [d/o 719]	- 60.17	43.02	0.72	9.03

data over Egypt with the SPW-R5 GGM, the classical RCR principle has been applied. For more details on the application of the RCR technique in geodesy, the interested reader is referred to Heiskanen and Moritz (1967). In physical geodesy, the RCR is considered one of the most widely applied methods to remove the long and very-short wavelengths contributions from the ground-based FA gravity anomalies, then after performing the LSC process, all the removed signals are restored back. Figure 6 depicts the flowchart of the RCR principle followed for the evaluation of the combined regional gravity model. In

the following subsections, the remove, compute, and restore steps are explicitly explained.

4.1. Remove Step

The effects of both the long and very-short wavelengths components of the gravity field should be removed from the terrestrial FA gravity anomalies in order to compute the residual field. Also, the data should be downward continued from their actual altitude to the geoid, in theory, or the surface of the Earth, in practice, by performing a downward continuation, but such a reduction step is out of scope of this work, and the interested reader is directed to Mansi et al. (2017) and Sansó and Sideris (2017). The syntheses of all the investigated GOCE-based GGMs truncated at d/o 200 are used to calculate the long wavelengths components. Furthermore, the very-short wavelengths contributions of the gravity signal were computed and removed exploiting the RTM method as shown in Fig. 7. The statistics of the

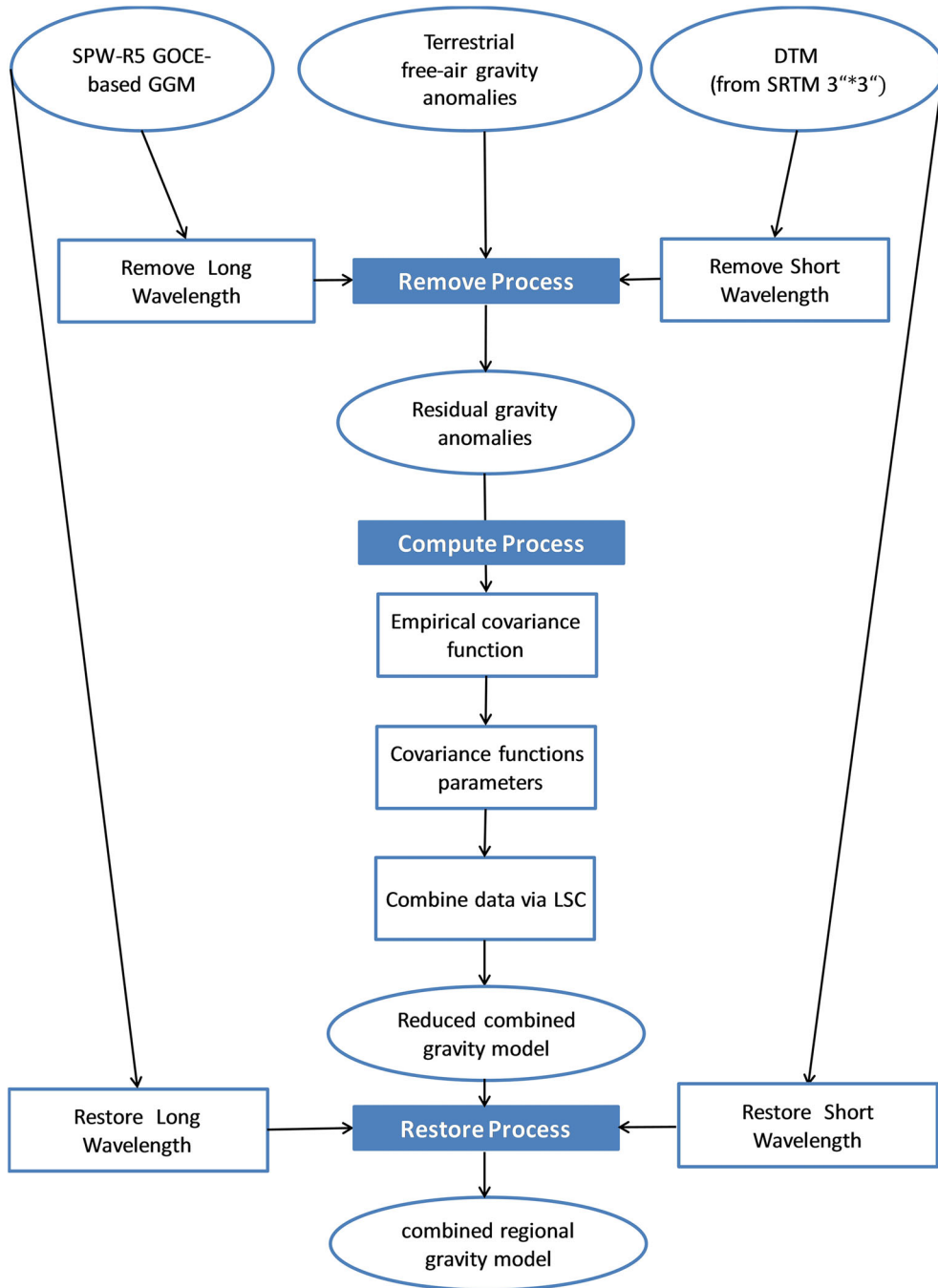


Figure 6
Flowchart describing the computation of the regional gravity model based on the RCR approach

observed and residual gravity anomalies are reported in Table 3.

The results clearly show that removing the long wavelengths components yields a substantial diminution of the data of about 53%, in terms of STD that dropped from 19.33 to 9.03 mGal. However, a further

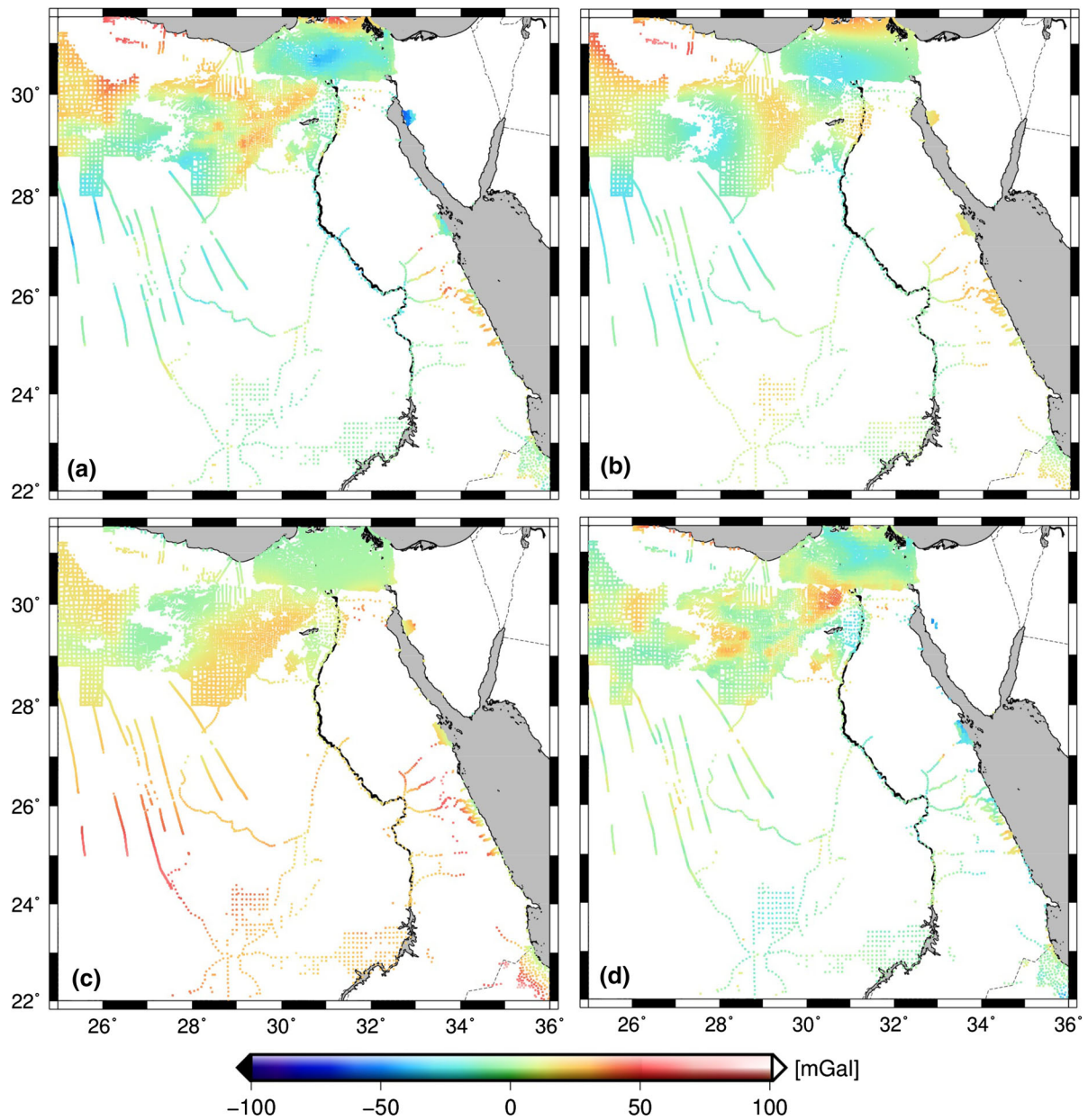


Figure 7

Data preparation (remove step) for the least-squares collocation (LSC). **a** The terrestrial FA anomalies; **b** the SPW-R5 (long wavelength component of the SPW GOCE solution); **c** the residual terrain model (RTM) and **d** the final reduced signals; unit [mGal]

reduction step that accounts for the RTM signal, i.e. the removal of the very-short wavelengths contributions, increased the variation of the data of about 58%, where the STD increased to 14.27 mGal; hence, additional improvements were not gained. Such abnormal results could be due to limitations in the

quality of the terrestrial gravity data provided by the Getech for Egypt. Consequently, in our study case, the RTM reduction is not a beneficial step and will not be accounted for within the development of the combined model. A similar behaviour was observed during the geoid computation of Sudan using Getech

Table 3

Statistics of the observed gravity anomalies, Δg_{obs} , reduced for the gravity anomalies, Δg_{GGM} of the SPW-R5 model and Δg_{RTM} of the residual terrain model; units [mGal]

Anomaly	Min	Max	Mean	STD
Δg_{obs}	– 62.399	72.80	– 2.76	19.33
$\Delta g_{\text{red}} = \Delta g_{\text{obs}} - \Delta g_{\text{GGM}}$	– 59.190	43.29	0.75	9.03
$\Delta g_{\text{red}} = \Delta g_{\text{obs}} - \Delta g_{\text{GGM}} - \Delta g_{\text{RTM}}$	– 97.960	65.45	– 8.35	14.27

data (Godah and Krynski 2015). Figure 7 reports the reduced gravity signals, the SPW-R5 GGM as well as the RTM contributions.

4.2. Compute Step (LSC and Covariance Information)

The LSC method, introduced to geodesy by Moritz (1972, 1978), is the most used stochastic modelling technique to perform an optimal linear estimation for gravity field parameters integrating different heterogeneous gravity data both in spatial and frequency domains (Barzaghi et al. 1993; Gildandoni et al. 2013). Krarup (1969) gave a formula for the best linear unbiased estimate of the signal (predictable stochastic part of a target quantity) in a Hilbert space with a reproducing kernel as follows:

$$S = C_{sl}(C_{ll} + C_{vv})^{-1} \cdot l \quad (2)$$

where S is the target quantity to be estimated from the vector of observations l , C_{sl} is the cross-covariance matrix that represents the signal covariance between the input signals l and the target quantity S . C_{ll} is the auto-covariance matrix of the observation vector, and C_{vv} is the variance-covariance matrix of the noise, which represents the standard error of the observed gravity anomalies (in practice a diagonal matrix). The covariance matrices C_{ll} and C_{vv} describe the statistical correlations of the signal and noise components, respectively.

One of the key advantages of the LSC is that it provides information about the errors alongside with the estimated regional gravity field and geoid models in forms of variances or even full variance-covariance matrix C_{ee} (Moritz 1989):

$$C_{ee} = C_{ss} - C_{sl}(C_{ll} + C_{vv})^{-1} \cdot C_{ls} \quad (3)$$

with C_{ss} represents the autocovariance matrix of the signal. The LSC toolbox used in this research is based on an algorithm developed by Tscherning et al. (1992).

Regarding the modelling step, the quality of the inversion of gravity data highly depends on the covariance function of the observations, i.e. the residual gravity signal (Knudsen 1987), as well as the covariance that accounts for the noise, if it exists (Tscherning 1985). Thereupon, such a task could be easily fulfilled by computing the empirical covariance function (see Fig. 8) using the residual gravity signal by the Empirical Covariance toolbox described in Sampietro et al. (2017).

Then, one of the well-known covariance functions that best fits the empirical covariance function computed from the data has to be chosen as the theoretical covariance function. In our case, the empirical covariance function estimated for the whole area of Egypt using the reduced gravity signal, Δg_{red} , is fitted with a set of n Bessel functions of the first-order and zero-degree (Kreh 2012; Braitenberg et al. 2016). Bessel functions exploit all the stochastic properties of the residual gravity signal to its upmost, which, in turn, reduces the mis-fitting/modelling between the empirical and theoretical covariance functions that can be mistakenly considered as coloured noise (Braitenberg et al. 2016).

As a consequence, the theoretical covariance function is built as a linear combination (with positive coefficients) of these n Bessel functions in the frequency domain, as shown in Fig. 8, exploiting the well-known relation between the 2D-power spectral densities and Bessel functions (Watson 1995), which guarantees to obtain a positive definite covariance matrix (Mansi 2016). Details on the theoretical aspects related to this procedure are

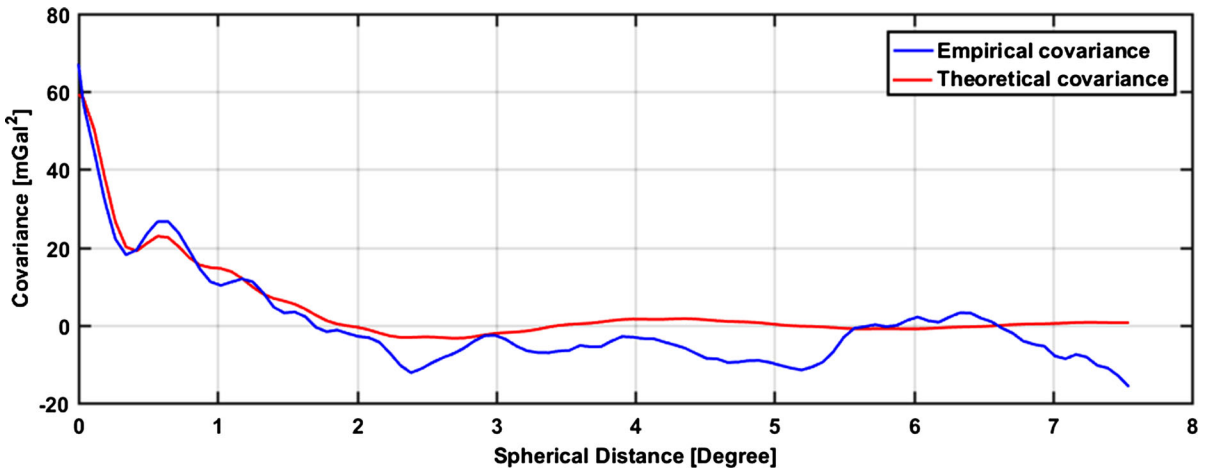


Figure 8
Empirical and analytical fitted covariance functions using different global geopotential models (GGMs); unit [mGal^2]

reported in Sampietro et al. (2017). Once the theoretical covariance function is estimated, it can be used to build the covariance matrix for the LSC procedure. In this step, the combination of the terrestrial data and the SPW-R5 GGM signal, synthesized at the same coordinates of terrestrial stations, can be straightforwardly performed if an estimate of the error of the SPW-R5 model is available.

The empirical and theoretical covariance functions, represented in Fig. 8, exhibit a good agreement up to 0.65° of spherical distance, before it reaches zero. These estimated parameters were then utilized to calculate the residual gravity anomalies on a regular grid of $5' \times 5'$ arc-minute spatial resolution. Having prepared all its constituents, the LSC was performed according to Eq. (2) to generate the targeted combined regional gravity field over Egypt.

4.3. Restore Step

At this point, the long and short wavelengths components of the gravity field can be restored and summed up to the residual gravity anomalies in order to obtain the full gravitational signal for the SPW-R5, DIR-R5, TIM-R5, and GOCO5S GGMs, as shown in Fig. 9. The former can be restored using the FA gravity field derived from the syntheses of the different GGMs truncated at d/o 200, whereas the

latter is recoverable from the EGM2008 model synthesized from d/o 201 to its maximum d/o, i.e. 719, in order to be compatible with the XGM2016. A note must be taken that the one does not need to restore the RTM signal as it has not been considered within the remove step because the reduced signal did not gain any improvements after taking it into consideration. The statistics of the differences between the various developed combined models and the XGM2016 model are reported in Table 4, where the SPW-R5-based regional combined model delivered the minimum STD value of 8.75 mGal, as expected. Therefore, the best combined regional gravity model for Egypt is computed on basis of the SPW-R5 model, displayed in Fig. 10, by summing up all the effects with the residual signal.

5. Combined Model Validation

Firstly, the Bouguer anomalies were computed by removing the gravitational effects of the topographic masses from the developed combined regional gravity model, computed by means of the GTE, as shown in Fig. 10, in order to validate the goodness of such a combined model. The estimated combined model in terms of FA and Bouguer anomalies (Fig. 10a, c) is

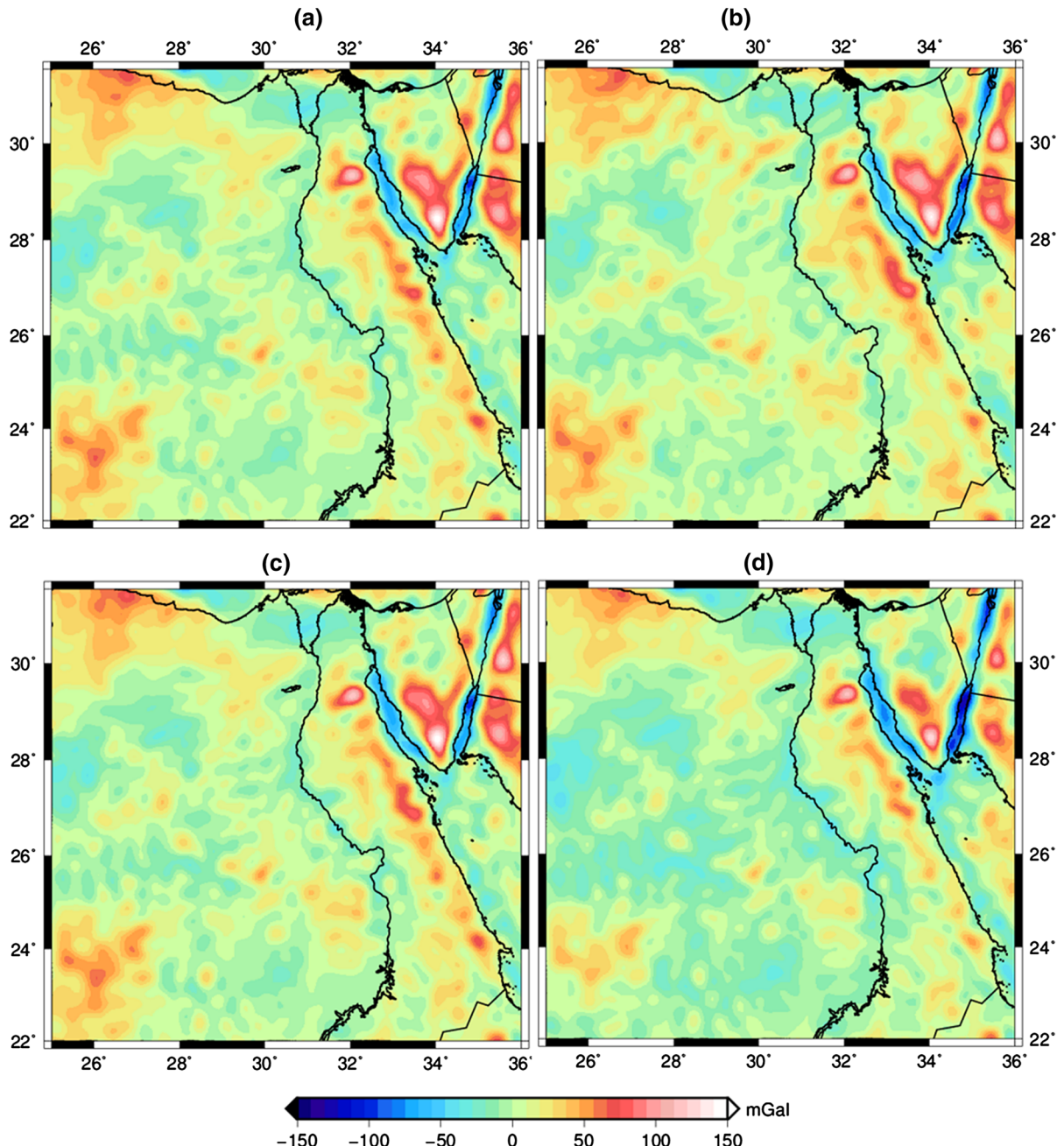


Figure 9

The restored signals using different global geopotential models (GGMs) models: **a** the SPW-R5; **b** the DIR-R5; **c** the TIM-R5; and **d** the GOCO5S GGM; unit [mGal]

compared to the XGM2016 model (Fig. 10b, d). Moreover, the differences evaluated by the combined regional gravity models with respect to the XGM2016 (see, Fig. 5) illustrated the lowest STD of

8.75 mGal for the SPW-R5-based combined model, see Table 4. A reminder must be made here, that the computational steps have been systematically repeated in order to compensate for the long wavelengths

Table 4

The statistics of the comparison between the XGM2016 model and the different combined models computed on basis of the SPW-R5, DIR-R5, TIM-R5, and GOCO5S GGMs; units [mGal].

Model	Min	Max	Mean	STD
XGM2016-SPW-R5	– 126.72	102.07	0.69	8.75
XGM2016-DIR-R5	– 118.97	104.38	1.29	9.59
XGM2016-TIM-R5	– 126.49	101.09	0.77	8.82
XGM2016-GOCO5S	– 100.25	121.78	2.04	10.46

contributions using the DIR-R5, TIM-R5, and GOCO5S models, whose restored signals with respect to the XGM2016 are characterized with STD values of 9.59, 8.82, and 10.46 mGal, respectively.

Hence, such differences could be seen as a direct reflection of the improvements gained from the produced combined regional gravity model, which has accounted for terrestrial data contribution, over the XGM2016 model, where such data were not used.

Furthermore, for an additional validation step, the radial average power spectrum of the combined gravity model, the XGM2016, and the SPW-R5 GGMs was calculated. As illustrated in Fig. 11, the power of the combined model is evidently higher in the short wavelengths band as a direct contribution of the terrestrial data. That is due to the fact that the combined model has more details since it contains short wavelengths attributes gained from the ground gravity data. The power of the XGM2016 model lies in between both models, the combined model and the SPW-R5, which is reasonable as it has a maximum d/o of 719.

A NorthEast–SouthWest cross-section, namely S1, was considered for a thorough wavelengths comparison between the combined, the SPW-R5, and the XGM2016 models, see Fig. 10. It can be easily noticed, from Fig. 12, that the SPW-R5 signal is the smoothest since it only contributes the long wavelengths. On the other hand, as mentioned earlier, the combined model retrieved more detailed short wavelengths as a direct contribution of terrestrial data. In contrast, the XGM2016 model, along the cross-section S1, looks smoother in comparison to the combined model since it solely has SHs until 719.

6. Forward Density Modelling

As a geophysical application, the combined regional gravity model was utilised to build a forward density model for the Delta region, located within the Northern Egypt, where dense data are available. The 2D forward gravity modelling was accomplished using the IGMAS+ software (Götze and Lahmeyer 1988; Schmidt et al. 2010).

The representative profile, named P1 (see Fig. 10), has been taken perpendicular to the general geological strike of the region oriented in the North–South direction. For the purpose of this research, the model setup initially contained several layers that were constrained by the interpretation of various deep seismic profiles (Makris et al. 1982; Marzouk 1988) with a fine-tuning applied on the geometry. The density values of the sedimentary layers were estimated based on the available drill wells studies executed over the Nile Delta area and those of the crust and upper mantle were derived from the P-wave seismic velocity by converting the velocities to density values using the approach of Christensen and Mooney (1995).

The model represents thick sedimentary basins from the North near the off-shore area (more than 8 km) that thin towards the South. The Northern part of the model shows a thin crust (≈ 24 km) beneath the coastal line of the Mediterranean Sea, with the crustal thickness increasing toward the South, reaching about 32 km (see Fig. 13).

The original density model proposed by Saleh (2012) was constructed without using any satellite gravity data. The calculated Bouguer anomaly represented as a black solid line in Fig. 13 served as a reference model in order to compare these estimated by the combined gravity model and the XGM2016 GGM.

The original model geometry and densities (Saleh 2012) were kept fixed and subsequently, the Bouguer anomaly of the combined regional gravity model was forward-calculated. The modelled signals almost perfectly match the observed gravity values with a STD of 7.0 mGal for the residuals evaluated for the observed and modelled signals. In contrast, the XGM2016 anomalies fit the general trend of the

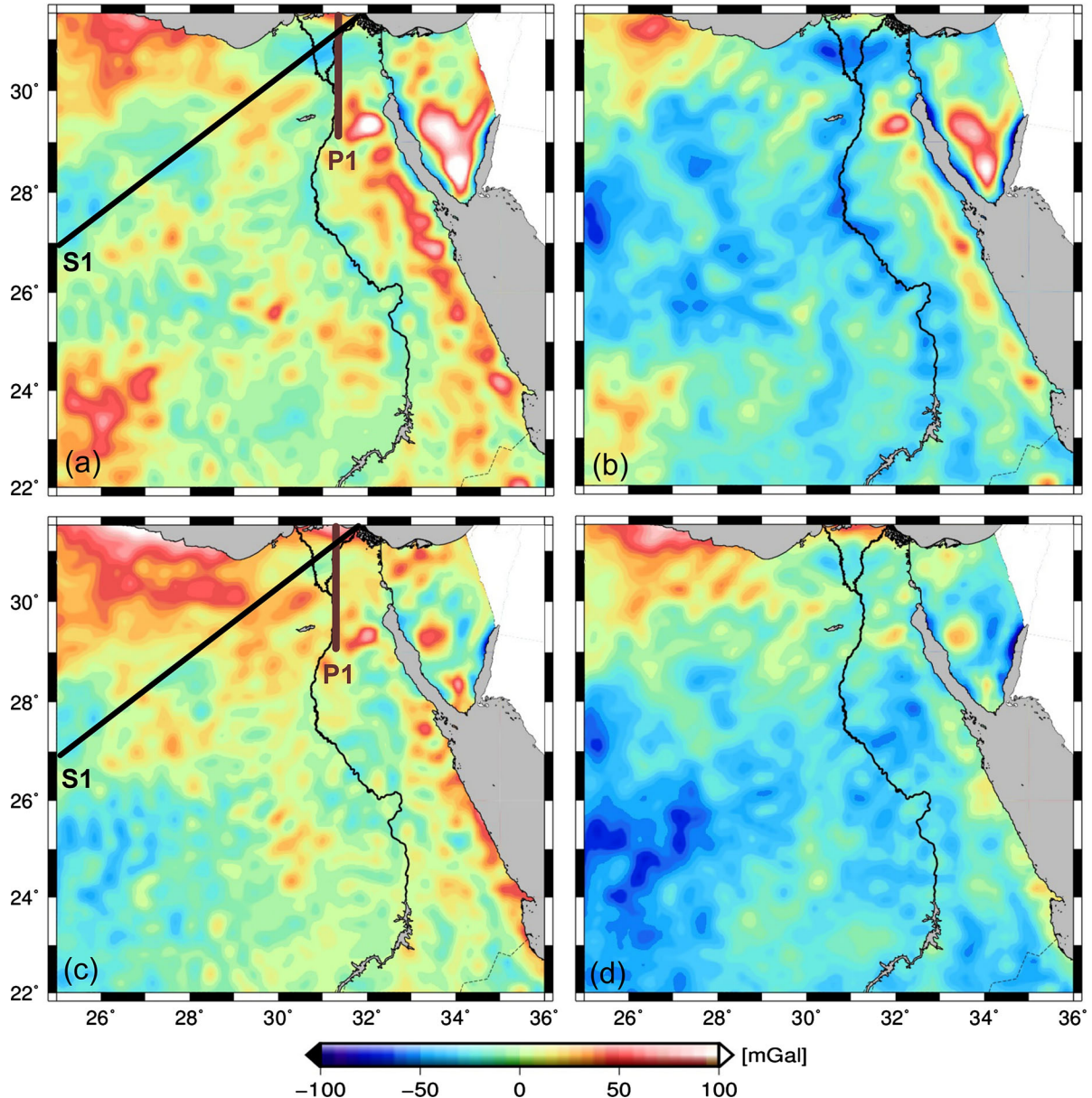


Figure 10

Comparison of the combined regional gravity model with the XGM2016 global geopotential model (GGM). **a** The free-air gravity anomalies according to our combined model, **b** the free-air gravity anomalies synthesised from the XGM2016 GGM, **c** the Bouguer anomalies (i.e. free-air anomalies reduced by the topographic effect) computed by the combined model, and **d** the Bouguer anomalies retrieved by the XGM2016 GGM. The brown line P1 shows the location of the profile described in Sect. 5 and the black line S1 displays the location of the NorthEast–SouthWest cross-section described in Fig. 12; unit [mGal]

observed data but with a higher STD equivalent to 18.0 mGal.

The produced mass deficit associated with the XGM2016 can be compensated by an increase in the

crustal and sediment density values or a decrease in the crustal and sediment thickness. However, such scenarios lead to an unrealistic crustal structure, which deviates from the density model of Saleh

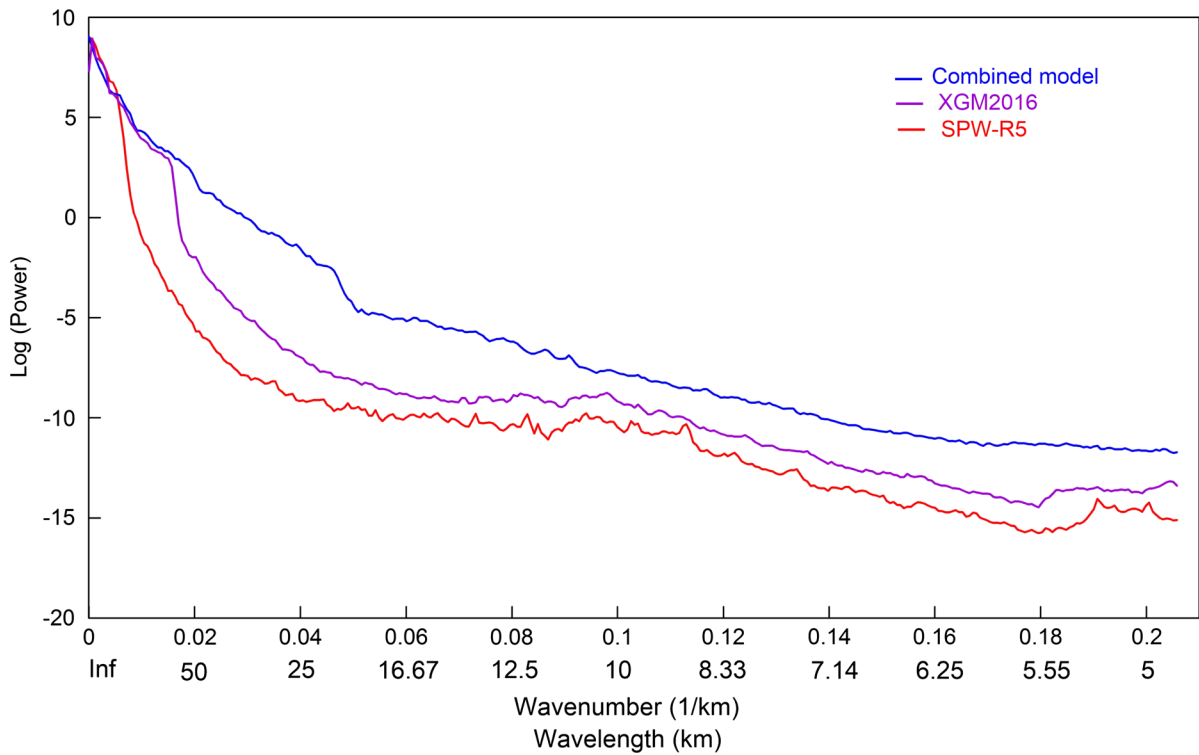


Figure 11

The Spectral representation of the combined model (blue), the XGM2016 model (purple), and the SPW-R5 global geopotential model (red); unit [Log(Power)]

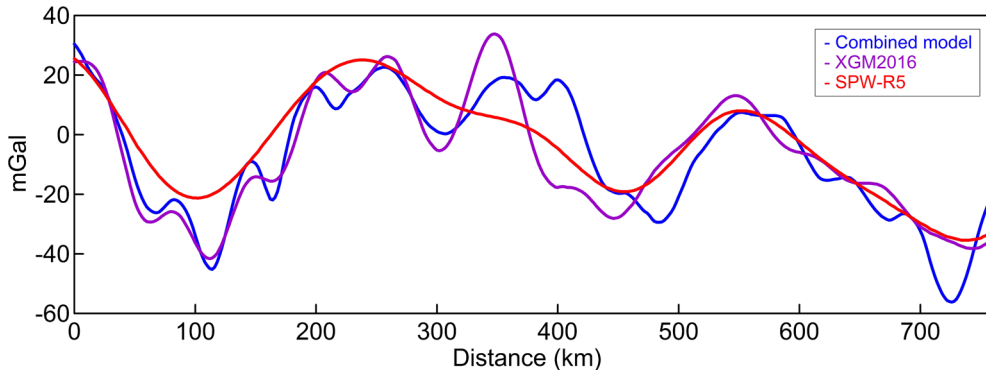


Figure 12

The differences between the combined model, the XGM2016, and the SPW-R5 global geopotential model along the NorthEast–SouthWest profile; unit [mGal]

(2012) that is seismically constrained. We aim to test the combined model with the existing model without any changes. The displayed anomalies from the combined model along the cross-section present a

good agreement with the well-constrained density model (Saleh 2012).

For our combined regional gravity model, the contribution of the terrestrial gravity measurements improved the gravity signals in comparison with the

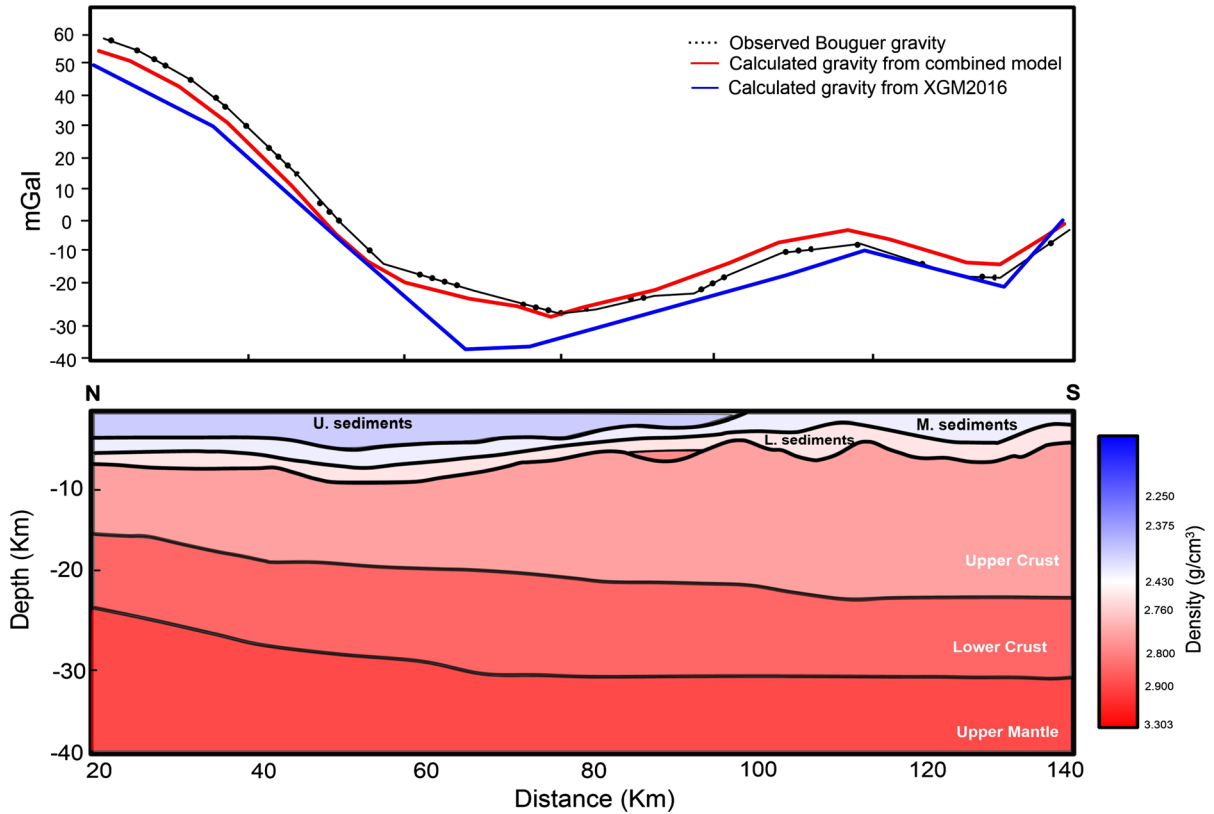


Figure 13

A vertical cross-section of a 3D density model from the P1 (North–South) profile over the Nile Delta region (P1). The thin solid black line is the measured gravity anomaly, the red solid line is the modelled gravity signal using the combined gravity model, and the blue solid line is the calculated gravity using the XGM2016 model. The Geometry and the density values of the model were retrieved from Saleh (2012)

XGM2016 model over the study region, since it has been generally developed using only a limited number of terrestrial gravity points, over Egypt.

7. Conclusion

A new combined regional gravity model has been developed for Egypt utilizing the recently made available terrestrial FA gravity anomalies integrated with the satellite gravity data. The terrestrial data used in this study, characterized with consistent gravity and height values, were exploited for the first time over the Egyptian territory. A quality control analysis has been done, for these terrestrial data, in order to exclude the gravity points, which have large discrepancies with respect to the SRTM-based DTM heights and/or positions in order to produce a

homogeneous dataset that is used for the development of the combined gravity field modelling.

With regard to the investigated GOCE-based gravity data, namely the SPW-R5, DIR-R5, TIM-R5, and GOCO05 GGMs, the space-wise solution, namely the SPW-R5, synthesized up to a SH d/o 200, is found to be the best model to closely approximate the gravity field over Egypt, especially in terms of the long wavelengths components. Accordingly, the classical RCR method and LSC technique have been applied in order to reduce the order of magnitude of the terrestrial FA gravity observations and afterwards integrate them with satellite gravity data.

Correspondingly, a combined model in terms of FA anomalies has been developed and compared with respect to the state-of-art XGM2016 model, which was developed using limited number of terrestrial gravity stations in Egypt, whose performance has

been thoroughly investigated. In order to test the combined gravity model, the Bouguer anomaly data, which were calculated from the FA signal, synthesized from the combined model, were forward-modeled using the IGMAS+ 3D modelling along a transversal profile, P1, crossing the Nile Delta area from North to South.

The modelled gravity signals, derived from the calculated combined gravity model, are in a good agreement with the observed gravity signals producing residuals characterized with a low STD equivalent to 7.0 mGal compared with the residuals of the XGM2016 that exhibited a STD of 18.0 mGal. This emphasizes that the developed combined regional gravity model delivers significant improvements over the XGM2016 model as a result of jointly exploiting both the satellite and a large number of terrestrial gravity observations. The combined model would definitely be of added-value for geophysical and geodetic applications where no or only sparse ground data are available. In addition, the method may be useful when combining other heterogeneous datasets of different resolution, e.g. onshore gravity data with offshore satellite data.

Acknowledgements

The present work has been supported by the German Academic Exchange Service (DAAD). We would like to thank Basem Elsaka (University of Bonn, Germany) for the helpful discussion. The authors also would like to thank Getech UK for providing the terrestrial gravity data over Egypt. The spatial representations of the results have been plotted using the GMT5 (Generic Mapping Tools) software (Wessel et al. 2013). The spherical harmonic syntheses have been computed using the GEOEGM module of the GRAVSOFT software (Tscherning et al. 1992).

REFERENCES

- Abd-Elmotaal, H. (2008). Determination of the geoid in Egypt using heterogeneous geodetic data. *NRIAG Journal of Geophysics*, special issue, 507–531.
- Abd-Elmotaal, H., Seitz, K., Kühtreiber, N., & Heck, B. (2018). AFRGDB_V2.0: The gravity database for the geoid determination in Africa. In *The international association of geodesy symposia* (pp. 1–10). Berlin, Heidelberg: Springer. https://doi.org/10.1007/1345_2018_29.
- Alnaggar, D. (1986). Gravimetric geoid for Egypt using high-degree tailored reference geopotential model. Ph.D. dissertation, Cairo University, Egypt.
- Arrell, K., Wise, S., Wood, J., & Donoghue, D. (2008). Spectral filtering as a method of visualising and removing striped artefacts in digital elevation data. *Earth Surface Processes and Landforms*, 33(6), 943–961. <https://doi.org/10.1002/esp.1597>.
- Barzaghi, R., Fermi, A., Tarantola, S., & Sansó, F. (1993). Spectral techniques in inverse stokes and Overdetermined problems. *Surveys in Geophysics*, 14(4), 461–475. <https://doi.org/10.1007/BF00690572>.
- Bomfim, E. P., Braatenberg, C., & Molina, E. C. (2013). Mutual evaluation of global gravity models (EGM2008 and GOCE) and terrestrial data in Amazon Basin, Brazil. *Geophysical Journal International*, 195(2), 870–882. <https://doi.org/10.1093/gji/ggt283>.
- Braatenberg, C., Sampietro, D., Pivetta, T., Zuliani, D., Barbagallo, A., Fabris, P., Rossi, L., Julius F., & Mansi, A. H. (2016). Gravity for detecting caves: Airborne and terrestrial simulations based on a comprehensive Karstic Cave benchmark. *Pure and Applied Geophysics*, 173(4), 1243–1264. <https://doi.org/10.1007/s00024-015-1182-y>.
- Brockmann, J. M., Zehentner, N., Höck, E., Pail, R., Loth, I., Mayer-Gürr, T., & Schuh, W.-D. (2014). EGM-TIM-RL05: An independent geoid with centimeter accuracy purely based on the GOCE mission. *Geophysical Research Letters*, 41(22), 8089–8099. <https://doi.org/10.1002/2014GL061904>.
- Bruinsma, S. L., Förste, C., Abrikosov, O., Marty, J.-C., Rio, M.-H., Mulet, S., & Bonvalot, S. (2013). The new ESA satellite-only gravity field model via the direct approach. *Geophysical Research Letters*, 40, 3607–3612. <https://doi.org/10.1002/grl.50716>.
- Capponi, M., Mansi, A. H., & Sampietro, D. (2017). Improving the computation of the gravitational terrain effect close to ground stations in the GTE software. *Studia Geophysica et Geodaetica*, 2017, 1–17. <https://doi.org/10.1007/s11200-017-0814-3>.
- Christensen, N. I., & Mooney, W. D. (1995). Seismic velocity structure and composition of the continental crust: A global view. *Journal of Geophysical Research*, 100(B6), 9761–9788. <https://doi.org/10.1029/95JB00259>.
- Dawod, G. M. (2008). Towards the redefinition of the Egyptian geoid: Performance analysis of recent global geoid and digital terrain models. *Journal of Spatial Science*, 53(1), 31–42. <https://doi.org/10.1080/14498596.2008.9635133>.
- Drinkwater, M. R., Floberghagen, R., Haagmans, R., Muñiz, D., & Popescu, A. (2003). GOCE: ESA's first earth explorer core mission. In: G. Beutler, M.R. Drinkwater, R. Rummel, & R. Von Steiger (Eds.), *Earth Gravity Field from Space—from sensors to earth sciences*. Space Sciences Series of ISSI, Vol. 17. Dordrecht: Springer. https://doi.org/10.1007/978-94-017-1333-7_36.
- European GOCE Gravity-Consortium (2010). GOCE level 2 product data handbook, GO-MA-HPF-GS-0110, Issue 4.2. Noordwijk: European Space Agency. http://earth.esa.int/pub/ESA_DOC/GOCE/Product_Data_Handbook_4.1.pdf.
- Fairhead, J. D., Watts, A. B., Chevalier, P., El-Haddadeh, B., Green, C. M., Stuart, G. W., Whaler, K. A., & Whindle, I. (1988). African gravity project. In *GETECH, Department of Earth Sciences, University of Leeds, University of Leeds Industrial Services Ltd., Leeds, UK*.

Regional Gravity Field Model of Egypt Based on Satellite

- Farr, Tom. G., Rosen, P. A., Caro, E., Crippen, R., Duren, R., Hensley, S., Kobrick, M., Paller, M., Rodriguez, E., Roth, L., Seal, D., Shaffer, S., Shimada, J., Umland, J., Werner, M., Oskin, M., Burbank, D., & Alsdorf, D. (2007). The shuttle radar topography mission. *Reviews of Geophysics*, 45(2). <https://doi.org/10.1029/2005RG000183>.
- Forsberg R. (1984). Study of terrain reductions, density anomalies and geophysical inversion methods in gravity field modelling. In *Report 355, Department of Geodetic Science and Surveying*. Columbus: Ohio State University. <http://www.dtic.mil/docs/citations/ADA150788>.
- Förste, C., Bruinsma, S., Abrikosov, O., Flechtner, F., Marty, J. C., Lemoine, J. M., Dahle, C., Neumayer, H., Barthelmes, F., König, R., & Biancale, R. (2014). EIGEN-6C4—the latest combined global gravity field model including GOCE data up to degree and order 1949 of GFZ Potsdam and GRGS Toulouse. In *EGU general assembly conference abstracts*, Vol. 16, Vienna. <https://doi.org/10.5880/icgem.2015.1>.
- Gatti, A., Reguzzoni, M., Sansò, F., & Venuti, G. (2013). The height datum problem and the role of satellite gravity models. *Journal of Geodesy*, 87(1), 15–22. <https://doi.org/10.1007/s00190-012-0574-3>.
- Gatti, A., Reguzzoni, M., Migliaccio, F., & Sansò, F. (2016). Computation and assessment of the fifth release of the GOCE-only space-wise solution. Thessaloniki, Greece, GGHS 2016: Presented at the 1st Joint Commission 2 and IGFS Meeting, 19-23 September 2016. <https://doi.org/10.13140/RG.2.2.28625.94569>.
- Gilardoni, M., Reguzzoni, M., & Sampietro, D. (2013). A least-squares collocation procedure to merge local geoids with the aid of satellite-only gravity models: The Italian/Swiss geoids case study. *Bollettino di Geofisica Teorica e Applicata*, 54(4), 303–319. <https://doi.org/10.4430/bgta0111>.
- Gilardoni, M., Reguzzoni, M., & Sampietro, D. (2016). GECO: a global gravity model by locally combining GOCE data and EGM2008. *Studia Geophysica et Geodaetica*, 60(2), 228–247. <https://doi.org/10.1007/s11200-015-1114-4>.
- Godah, W., & Krynski, J. (2015). Comparison of GGMs based on one year GOCE observations with the EGM2008 and terrestrial data over the area of Sudan. *International Journal of Applied Earth Observation and Geoinformation*, 35(A), 128–135. <https://doi.org/10.1016/j.jag.2013.11.003>.
- Götze, H., & Lahmeyer, B. (1988). Application of three-dimensional interactive modeling in gravity and magnetics. *Geophysics*, 53(8), 1096–1108. <https://doi.org/10.1190/1.1442546>.
- Hanafy, M. S., & El Tokhey, M. A. (1993). Simulation studies for improving the geoid in Egypt. In *Geodesy and Physics of the Earth*, 60(2), 153–158. Berlin, Heidelberg: Springer. ISBN:978-3-642-78149-0.
- Heiskanen, W. A., & Moritz, H. (1967). *Advanced physical Geodesy*. San Francisco: W.H. Freeman and Company.
- Kaula, W. M. (1966). Theory of satellite Geodesy. Blaisdell Publishing Company, Waltham, Republished 2000 by Dover Publications Inc., Mineola.
- Knudsen, P. (1987). Estimation and modelling of the local empirical covariance functions using gravity and satellite altimeter data. *Bulletin géodésique*, 61(2), 44, 145–160. <https://doi.org/10.1007/BF02521264>.
- Krarup, T. (1969). A contribution to the mathematical foundation of physical geodesy. *Geodetic Institute Copenhagen*, 44(80), 44.
- Kreh, M. (2012). Bessel functions. Lecture notes, Project for the Penn State StateGöttingen summer school on number theory. <http://www.math.psu.edu/papikian/Kreh.pdf>.
- Makris, J., Weigel, W., Moeller, L., Goldform, P., Behle, A., Stoefen, B., Allam, A., Maamoun, M., Delibasis, N., Perissaratis, K., Avedik, F., & Giese, P. (1982). Deep seismic soundings in Egypt, Part 1: The Mediterranean Sea between Crete-Sidi Barani and the coastal areas of Egypt. Internal Report, University of Hamburg, FRG.
- Mansi, A. H. (2016). Airborne gravity field modelling. Ph.D. dissertation, Politecnico di Milano, Italy.
- Mansi, A. H., Capponi, M., & Sampietro, D. (2017). Downward continuation of airborne gravity data by means of the change of boundary approach. *Pure and Applied Geophysics*, 2017, 1–12. <https://doi.org/10.1007/s00024-017-1717-5>.
- Marzouk, I. A. (1988). Study of crustal structure of Egypt deduced from deep seismic and gravity data. Ph.D. dissertation, University of Hamburg, FRG.
- Mayer-Gürr, T., Pail, R., Gruber, T., Fecher, T., Rexer, M., Schuh, W.-D., Kusche, J., Brockmann, J.-M., Rieser, D., Zehentner, N., Kvas, A., Klinger, B., Baur, O., Höck, E., Krauss, S., & Jäggi, A. (2015). The combined satellite gravity field model GOCO05s. In *Presented at EGU General Assembly 2015*, Vienna, 12–17 April.
- Moritz H. (1972). Advanced least-squares methods. In *Reports of the Department of Geodetic Science, No. 175*. Columbus, USA: The Ohio State University.
- Moritz, H. (1978). Least-squares collocation. *Reviews of Geophysics*, 16(3), 421–430. <https://doi.org/10.1029/RG016i003p00421>.
- Moritz, H. (1989). *Advanced physical geodesy*. Karlsruhe: Wichmann Verlag.
- Pail, R., Goiginger, H., Mayrhofer, R., Schuh, W.-D., Brockmann, J. M., Krasbutter, I., Höck, E., & Fecher, T. (2010). GOCE gravity field model derived from orbit and gradiometry data applying the time-wise method. In *The ESA Living Planet Symposium*, Vol. 28, Bergen, 28 June–2 July 2010.
- Pail, R., Bruinsma, S., Migliaccio, F., Förste, C., Goiginger, H., Schuh, W.-D., Höck, E., Reguzzoni, M., Brockmann, J. M., Abrikosov, O., Veichters, M., Fecher, T., Mayrhofer, R., Krasbutter, I., Sansò, F., & Tscherning, C. C. (2011). First GOCE gravity field models derived by three different approaches. *Journal of Geodesy*, 85(819), 845–860. <https://doi.org/10.1007/s00190-011-0467-x>.
- Pail, R., Fecher, T., Barnes, D., Factor, J., Holmes, S., Gruber, T., & Zingerle, P. (2016). The experimental gravity field model XGM2016. In *International symposium on gravity, geoid and height system 2016*, Thessaloniki, Greece.
- Pavlis, N. K., Holmes, S. A., & Kenyon, S. C. (2008). An earth gravitational model to degree 2160: EGM2008. In *General assembly of the European geosciences union 2008*, Vienna, Austria. http://mt.dgfi.tum.de/typo3_mt/fileadmin/2kolloquium_muc/2008-10-08/Bosch/EGM2008.pdf.
- Reigber, C., Lühr, H., & Schwintzer, P. (1999). The CHAMP geopotential mission. *Bollettino di Geofisica Teorica ed Applicata*, 40(3–4), 285–289. http://www3.ogs.trieste.it/bgta/pdf/bgta40.3.4._REIGBER1.pdf.
- Rummel, R. (2010). GOCE: Gravitational gradiometry in a satellite. In: W. Freedman, F.M.Z. Nashed, & T. Sonar (Eds.), *Handbook of geomathematics*, Vol. 2 (pp. 93–103). Berlin: Springer. https://doi.org/10.1007/978-3-642-01546-5_4.

- Saleh, S. (2012). 3D crustal structure and its tectonic implication for Nile delta and greater Cairo regions, Egypt, from geophysical data. *Acta Geodaetica et Geophysica Hungarica*, *47*(4), 402–429, Akadémiai Kiadó. <https://doi.org/10.1556/AGeod.47.2012.4.3>.
- Sampietro, D., Capponi, M., Mansi, A. H., Gatti, A., Marchetti, P., & Sansò, F. (2017). Space-Wise approach for airborne gravity data modelling. *Journal of Geodesy*, *91*(5), 535–545. <https://doi.org/10.1007/s00190-016-0981-y>.
- Sampietro, D., Capponi, M., Triglione, D., Mansi, A. H., Marchetti, P., & Sansò, F. (2016). GTE: a new software for gravitational terrain effect computation: Theory and performances. *Pure and Applied Geophysics*, *173*(7), 2435–2453. <https://doi.org/10.1007/s00024-016-1265-4>.
- Sampietro, D., Mansi, A. H., & Capponi, M. (2018). Moho depth and crustal architecture beneath the Levant Basin from Global Gravity Field Model. *Geosciences*, *8*(6), 200–214. <https://doi.org/10.3390/geosciences8060200>.
- Sampietro, D., Mansi, A. H., & Capponi, M. (2018). A new tool for airborne gravimetry survey simulation. *Geosciences*, *8*(8), 292–301. <https://doi.org/10.3390/geosciences8080292>.
- Sansò F., & Sideris M.G. (2017). Geodetic boundary value problem: The equivalence between Molodensky's and Helmert's solutions. Springer. ISBN: 3319463586 and 9783319463582.
- Schmidt, S., Götz, H.-J., Fichler, C., & Alvers, M. (2010). IGMAS+ a new 3D Gravity, FTG and magnetic modeling software. In: A. Zipf, K. Behncke, F. Hillen, & J. Schefermeyer (Eds.), *Die Welt Im Netz* (pp. 57–63). Geoinformatik 2010, Kiel, 17.3.–19.3.2010.
- Shih, H., Hwang, C., Barriot, J. P., Mouyen, M., Corréia, P., Lequeux, D., & Sichoix, L. (2015). High-resolution gravity and geoid models in Tahiti obtained from new airborne and land gravity observations: data fusion by spectral combination. *Earth, Planets and Space*, *67*(1), 124–140. <https://doi.org/10.1186/s40623-015-0297-9>. <https://earth-planets-space.springeropen.com/articles/10.1186/s40623-015-0297-9>.
- Tapley, B. D., Bettadpur, S., Watkins, M., & Reigber, C. (2004). The gravity recovery and climate experiment: Mission overview and early results. *Geophysical Research Letters*, *31*(9), 1–4. <https://doi.org/10.1029/2004GL019920>.
- Tscherning, C.C. (1985). Local approximation of the gravity potential by least squares collocation. In K.P. Schwarz (Ed.), *Local gravity field approximation* (pp. 277–361). The University of Calgary, Alberta, No. 60003.
- Tscherning, C.C., Forsberg, R., & Knudsen, P. (1992). The GRAVSOFT package for geoid determination. In *Proceedings of the 1st continental workshop on the Geoid in Europe* (pp. 327–334). Research Institute of Geodesy, Topography and Cartography, Prague.
- Walker, W., Kellndorfer, J. M., & Pierce, L. (2007). Quality assessment of SRTM C- and Xband interferometric data: Implications for the retrieval of vegetation canopy height. *Remote Sensing of Environment*, *106*(4), 428–448. <https://doi.org/10.1016/j.rse.2006.09.007>.
- Watson, G.N. (1995). *A treatise on the theory of Bessel functions* (2nd ed.). Montpelier: Cambridge University Press. ISBN 0521483913 and 9780521483919.
- Wessel, P., Smith, W. H. F., Scharroo, R., Luis, J. F., & Wobbe, F. (2013). Generic mapping tools: Improved version released. *Eos, Transactions American Geophysical Union*, *94*(5), 409–410. <https://doi.org/10.1002/2013EO450001>.
- Yoder, C. F., Williams, J. G., Dickey, J. O., Schutz, B. E., Eanes, R. J., & Tapley, B. D. (1983). Secular variation of Earth's gravitational harmonic J2 coefficient from Lageos and nontidal acceleration of Earth rotation. *Nature*, *303*, 757–762. <https://doi.org/10.1038/303757a0>.
- Zaki, A., Mansi, A. H., Selim, M., Rabah, M., & El-Fiky, G. (2018). Comparison of satellite altimetric gravity and global geopotential models with shipborne gravity in the red sea. *Marine Geodesy*, *41*(3), 258–269. <https://doi.org/10.1080/01490419.2017.1414088>.

(Received December 12, 2017, revised August 14, 2018, accepted August 20, 2018)